

Gold Nanoparticle Coated Biocompatible Polymeric Matrix Mesh Plasticizers Embedded over Polyvinyl Chloride Plastic Porous Grid: Designed Reusable Microbial Screening Mask and Its Application

R. Das¹* and S. Mondal¹*

¹ School of Health and Medical Sciences, Adamas University, Kolkata, West Bengal 700126, India

Received 27 September 2023; revised 29 November 2023; accepted 12 December 2023; published online 25 March 2024

ABSTRACT. Under severe pandemic conditions, any airborne microbe, including severe acute respiratory syndrome coronavirus 2 (SARS-CoV-2), leads to increased fatality if physical screening is compromised. Therefore, an investigation was carried out to design a reusable screening mask that could promise the highest safety and be compatible with users. After going through the analytical and clinical investigation, the design and the work quality are confined to the ground version. To initiate top quality mask screener design of high-tech gold nanoparticles (AuNPs) hydroxyethyl methacrylate (HEMA) composite mask, safety evaluation data from all masks were collected. The porous polyvinyl chloride (PVC) circular grid frame was coated with a gold metallic nano particles layer, and the flexible adhesive polymeric matrix mesh plasticizers polyethylene terephthalate (PET) was used to coat bed on each grid, as a design. In-vitro quantitative analysis process assembly of bio-contaminant and specific matter was developed, in which breathed/vacuumed air was passed via fractional screening cone adhesive edged stumbling block route for final pure contaminant free air. The vacuumed air was collected through the adhesive slide, and microbial growth and particular matter were analysed and discovered to be best compared to conventional filter masks. Gold coat film entrapment tests with colony density were performed through Fourier transform infrared spectroscopy (FTIR), and virus crystal structure analysis was done through an X-ray diffractometer. Clinical investigations of this development were done with 50 volunteers. The research demonstrates the advantages of the AuNPs HEMA composite reusable mask design comparatively best over other mask designs regarding microbiological screening and lab safety, and it may be helpful to stand against biological warfare.

Keywords: airborne microbe, AuNPs HEMA composite mask, total microbial protection, clinical evaluation

1. Introduction

In the face of severe pandemic circumstances, such as the threat presented by airborne germs, especially the highly infectious severe acute respiratory syndrome coronavirus 2 (SARS-CoV-2) virus, the integrity of physical screening methods becomes critical. Individual safety is paramount, necessitating the development of new methods to create a reusable screening mask that provides the maximum degree of protection while staying user-friendly and biocompatible. The current study article offers the findings of an inquiry aimed at resolving this critical issue.

Since 2019, SARS-CoV-2 has mostly seen severe changes in preventative mode, with several mask designs for quality microbiological filtering entering the market in addition to saniti-

zation and vaccination (Chou et al., 2020; Chou et al., 2022; Loeb et al., 2022). Only coronavirus disease (COVID) is not a reason to consider masks, but in the future, there will be a persistent threat of biological conflicts and hospital-acquired diseases (Jeffer-son et al., 2008; Smith et al., 2016; Offeddu et al., 2017), which will directly explain the cause of pandemics via communicable resistant strains (Gandhi et al., 2006; Gel-manova et al., 2007; O'Donnell et al., 2010). LG Company created some thick screened filter masks in addition to various layered fabric or fibre screened masks such as N95, and surgical masks (MacIntyre et al., 2017; Abd-Elsayed and Karri, 2020; Allison et al., 2021). However, causality and casualties are not thoroughly investigated and managed. The increased colony density might be due to air moving or entering via the opening (Krzeminski et al., 2019; Atangana and Atangana, 2020; Chou et al., 2020). Furthermore, the screening was just for filtering reasons rather than neutralization. As a result, there is an additional requirement for such a covering as a screen, which can work in three ways: (a) comprehensive microbe screening, (b) neutralization of trapped microorganisms inside the screen, and (c) cleaning or flashing off microbial from the mask without affecting the filter matrix, mesh (MacIntyre et al., 2017; Abd-Elsayed and Karri, 2020; Allison et al., 2021; Grignoli et al.,

* Corresponding author. Tel.: +91-986-314-0842.

E-mail address: rdas.jupharmtech@gmail.com (R. Das).

* Corresponding author. Tel.: +91-967-439-2785.

E-mail address: sandip1706@yahoo.com (S. Mondal).

2021). Biocompatibility, compactness, and the hard casing of wearable and washable masks are other essential (Pang et al., 2022; Yang et al., 2022; Ye et al., 2022). So, for the creation of the filter, the designs of the screen (Rengasamy et al., 2015; Hutten, 2016; Neupane et al., 2019), as well as the materials utilized for the hard construction to create an integral infrastructure, have been informed. Furthermore, considerable attention was made on covering the inner porous grids with a compatible polymer matrix and appropriate metal ion-reinforced composites (Armentano et al., 2021). Besides, the intended screen and material integrity catch the 100% microbial air colonies and anchor them for a certain period of time, preventing these microbial colonies from dispersing elsewhere (Clase et al., 2020; Kumar and Parekh, 2020; Lin et al., 2021). Later phase, which may be simply drained and cleaned completely without the need of abrasive procedures (Ullah et al., 2020).

As a result, an extensive analytical and clinical investigation was conducted in response to the pressing demand for improved mask screener designs capable of giving top-tier safety. This endeavour has resulted in the creation of a cutting-edge high-tech mask made of gold nanoparticle (AuNPs) coated hydroxyethyl methacrylate (HEMA) composite that has been carefully tested for safety and efficacy. A porous polyvinyl chloride (PVC) circular grid frame is covered with a coating of gold metallic nanoparticle in this revolutionary mask design. Each grid is also outfitted with a flexible sticky polymeric matrix mesh plasticizer made of polyethylene terephthalate (PET). This all-encompassing approach to mask design and assembly seeks to give a comprehensive solution to air filtration and microbiological screening, as well as public health emergencies and biodefense.

2. Methodology

2.1. Microstructure Description of Plastic Porous Grid and Septum

For its hardness, PVC material is mostly employed for the branching of a circular grid based on a center septum constructed of polycarbonate (PC) materials. Porous PVC-branched circular grids are created in order to embed a porous adhesive polymeric layer on top of them. The scanning electron microscopy (SEM) images of PVC have been depicted in Figure 1. When the porous PVC circular grid frame was coated with a metallic nanoparticle layer, the flexible adhesive polymeric bed on each grid could be fastened permanently with exceptional electrostatic capabilities. Each polymeric etched grid was enhanced with gold metallic nanoparticle, tiny particles typically ranging in size from 1 to 100 nanometers, to provide friction on the entering air stream during inspiration. Furthermore, dust particles, airborne viruses, and bacteria are trapped.

Resin is the primary component of PVC. It is a white, brittle material that comes in the shape of granules or powder. PVC is currently replacing traditional building materials such as ceramics, metal, concrete, wood, rubber, and many others. A chemical process polymerizes vinyl chloride monomer to produce PVC.

PVC is a lightweight, robust, and abrasion-resistant material by nature. This versatile thermoplastic polymer is not affected by any inorganic chemicals. PVC is an excellent insulating material due to its high dielectric strength and vapour barrier capability. It is unaffected by extreme weather, stress, or corrosion. As a result, it is the preferred approach for a wide range of outdoor applications. Longevity is assured due to increased durability. PVC products have a high quantity of chlorine, causing them to self-extinguish. PVC may be made more flexible, softer, and bendable by adding plasticizers such as phthalate and PVC is naturally flame resistant. It has a high tensile strength and is inherently stiff. It is a low-cost and efficient choice.

Because PVC is inherently amorphous, it is easily mixed with various substances and chemicals (Akovali, 2012). Depending on the additives used in PVC manufacturing, a variety of features like as anti-mist, varied colours, elasticity, fire retardancy, flexibility, impact resistance, and microbe prevention may be added to goods. PVC offers good chemical and flame resistance, a high strength-to-weight ratio, and dielectric characteristics, in addition to superior tensile, flexural, and mechanical strength, minimal moisture absorption, and exceptional dimensional stability. PC's chemical structure, which is extremely strong, is the source of its strength. Its molecules contain a high density of highly strong connections, giving it extraordinary resistance. Another benefit is the variety of pressures and accidents that PC can sustain. PC is made by condensing bisphenol A [$\text{HO}-(\text{C}_6\text{H}_6)-\text{C}-(\text{CH}_3)_2-(\text{C}_6\text{H}_6)-\text{OH}$] with carbonic acid ($\text{HO}-\text{CO}-\text{OH}$) (Emblem, 2012).

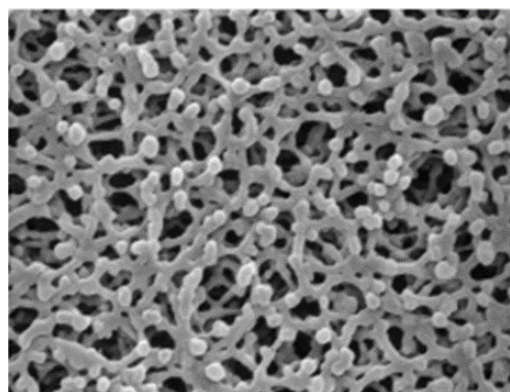


Figure 1. SEM image of PVC microstructure.

One of the most extensively used engineering thermoplastics, PC, is transparent and possesses remarkable durability, thermal stability, fire-resistant, vandal-proof, hardwearing insulating, lightweight, and easy to machine and dimensional stability (Edwards, 1998). There are transparent sheets of thermoplastic PC available. It is highly tough and absorbs very little moisture, making it resistant to both impact and water damage.

2.2. Preparation of the Polymeric Matrix Mesh Plasticizers

AuNPs were mixed with PET. Methylene diphenyl diisocyanate (MDI, a biological filler) was added to AuNPs to make

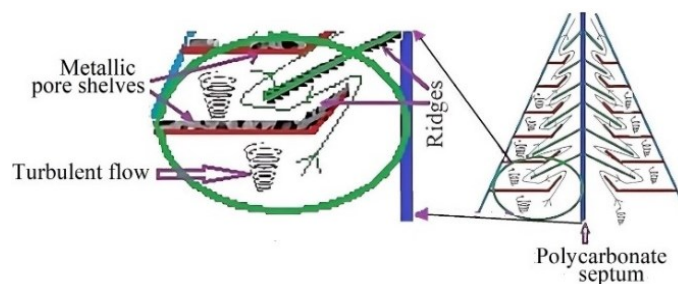


Figure 2. Inner designed structural integrity of filter cones with working principles.

reinforced AuNPs (RGNP), which was melted with PET resin to create PET/RGNP composites, which were then used to create plasticizers. After reinforcing AuNPs into resin PET through melting filler, it has a high strength and tensile of $\sigma_t = 55 \sim 75$ MPa (in normal, and after melting and re-crystallizing, it exceeds the density over the normal range of 1.455 g/cm^3) (Stearne and Ward, 1969).

Though the rheological properties of PET after melting tend to be non-Newtonian, the melt viscosity is more sensitive to the shear rate than to the temperature. During the processing, the processing fluidity of the polyester can be effectively improved by changing the shear rate. Incorporating distiller's grains (DG) also increases the shearing force (Chen et al., 2022). Hence, it possesses strong tensile, shear, hydrophobicity, and elastic qualities as a result.

2.3. Designing and Kinetics of Mesh Filter Assembly

Each hard plastic-based PC shelf is covered with biocompatible polymeric matrix mesh plasticizers, which are 2-hydroxyethyl methacrylate (2-HEMA) polymers (Zhang et al., 2012). HEMA has the qualities of initiating electrostatic forces and having the least adhesive and non-sticky properties for all airborne biological and non-biological nanoparticles dispersed in the air. HEMA plasticizer's outstanding surface features make it washing in somewhat turbulent water and reusable thanks to its prolonged adhesion capabilities. It has a viscosity of 0.0701 Pa at $20 \text{ }^\circ\text{C}$ and 0.005 Pa at $30 \text{ }^\circ\text{C}$, respectively. Aside from that, there are minimal mechanical shearing tendencies and modest thermal size changes. This inert polymer covering is glued and mechanically reinforced on PVC shelves. As shown in Figure 2, the two-cone mask filter is made up of the integrity of a PC frame at the axial clamp known as the septum and much gold (metallic) granular pore shelves covered with a thin film coating of HEMA plasticizer on centripetal and axial shelves.

As a result, there are multiple grids implanted with a thin coating of low-adhesive sticky cover across the whole inner cone structure of the shelves. Figure 3 shows the interior structure enlarged, revealing the inner architecture of the shelves. For efficient filtering, the inner planned structure is backed by the following operating logics.

2.4. Working Principle

The polluted air enters via the full cone with varied obstructive shelves while inhaling after wearing this integrated

filter device on the mask. A chaotic swirl is created here owing to structural impediments. The tumultuous whirl of air pollution flows in three dimensions across the whole surface of the shelves. Friction existed on the same side due to the ridges, groves of gold metal micro-granules, and grids. The numerous micro grids are aligned so that the micro-cone tips face the entrance of air streams, resulting in frictional filtration as well as particulate matter sticking to the plasticizer's bedding as it moves inside the nasal filter cones through the various stomas and apertures.

The polluted air will enter through the apertures of different gates between the shelves inherent structures during inhalation. The contaminated air will be turbulent at that moment, with particulate matter and any biological suspensions on it. As a result, the turbulent air will make contact with the full inner surface area 99% of the time and more than five times in each chamber. As a result of the sticky plasticizer, the particles are trapped simultaneously in each compartment based on the density of the contaminant and particle size.

As a result, screening occurs incrementally from the bottom to the top of the chambers. Simultaneously, air expiration causes the evacuation of these contaminated air particles by providing a pneumatic negative pressure of heated air and related speed. The nose cone might be cleaned with regular mild detergent by soaking for $5 \sim 10$ minutes, followed by standard tap water flash-washing.

2.5. Laboratory Evaluations

After gathering samples from each chamber and, lastly, from the filtrate air that comes out of the tip of the cone on the terminal zone of entry before going into the nasopharynx, the laboratory assessment would be performed. The route proposed for the pilot model was tested in the laboratory in vitro. There is a conventional air container/jar, a volume-velocity control vacuum pump, a fractional screening filter cone inside the chamber, and clear slides within the completed slide chamber.

2.6. Working Procedure

A smart vacuum pump is set up to control the quantified volume and pressure of air through the inlet, similar to our physiological in vivo breathing process of 400 mL for females and 500 mL for males per breath (tidal volume) at a rate of 12 times per minute, resulting in a minute ventilation rate of about 6 L of air per minute. At 4.5 to 6 mm Hg pulmonary pressure,

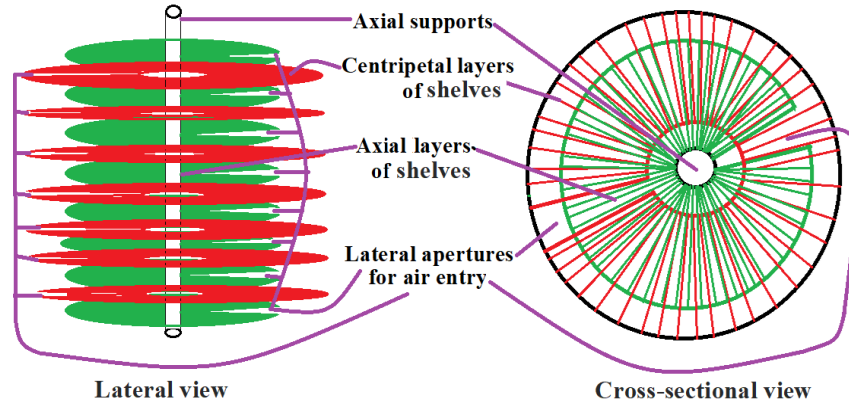


Figure 3. Three-dimensional inner engineering of shelves layer zones and air aperture position.

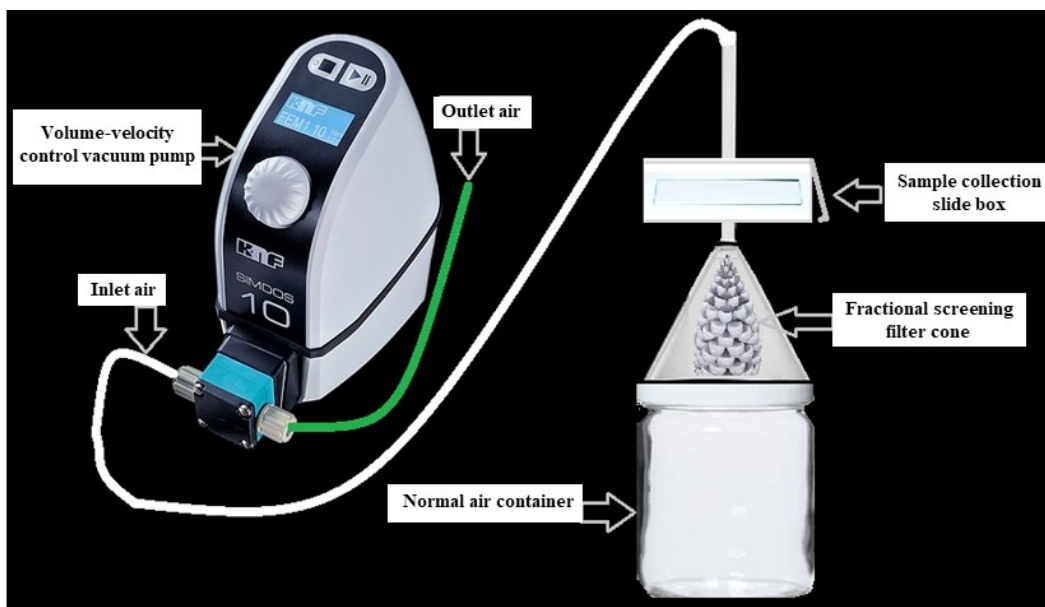


Figure 4. In-vitro quantitative analysis process assembly of bio-contaminant and particulate matter.

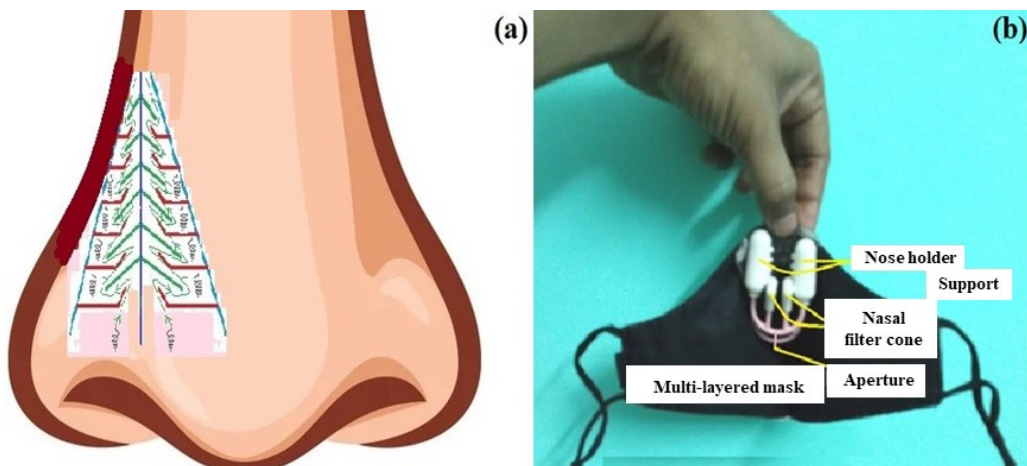


Figure 5. Pictures of (a) nasal cone filter location inside nose and (b) integrated gadget on mask to filter and remove all nano-bio contaminant and particle matters.

Table 1. Survey of Mask Operation Effectivity among 50 Volunteers of Senior Citizen, Young Athletes, and Normal Youth

Volunteer Group	Number of Volunteers	Average Recurrence of Respiratory Disease or SARS-CoV-2			Breathlessness, CVD, Allergic Reaction, Nasopharyngeal Discomfort, and Instant of Communicable Disease Retard	Performance Based on Force Exposure to SARS-CoV-2, Disease Manifestation, and Outcome after Wearing this Mask
		Before Wearing Mask [A]	After Wearing Mask [B]	Difference between A-B Stage, Disease Retention Time		
Senior Citizen	37/50	3 times	0	Least	Reduce to average 22%	0% (Zero)
Young Athletes	8/50	2 times	0	Least	Reduce to average 36%	0% (Zero)
Normal Youth	5/50	4 times	0	Least	Reduce to average 0%	0% (Zero)

the intake air terminal alternately pushes and pulls air in the usual physiological rhythm. The second terminal, on the other hand, is the outflow for the full collected air volume. Occasionally, the container must be replaced throughout this procedure to gather new ambient air. A pump controls the inhaled air volume, allowing it to strike the slide (which is located within the slide box) with the tip positioned vertically above the fractional screening chamber (Figure 4). Following the procedure, the slide was removed and examined under the microscope.

2.7. Fixing of Designed Filter Inside a Multilayered Cloth Mask

Many individuals utilized multilayered fabric masks, especially when a major epidemic was identified (OECD, 2020). Additionally, when pollutants are significantly more aggressive, respiratory issues or allergic responses may arise. The main disadvantage is that the multi-layered mask requires daily cleaning and creates breathing difficulties (Rosner, 2020). However, if two nostrilinserted gadgets with a conical screening inner structure are constructed on a basic single-layered mask, the filtering of biocontaminants and particulate matter/dust in the air may be highly regulated.

Both nasal cones are located with one side connected to the mask and the other side free to fit within both nostrils Figure 5a. After 7 ~ 14 days of regular breathing, the mask may be washed by simply dipping it in detergent, because the screening mechanism not only filters the air but also continually removes bio-contaminants and particulate debris. The integrated gadget of the screening filters, which eliminates all nano-biocontaminants and particle matters, was made to make it comfortable and compliant Figure 5b.

2.8. Analytical Investigation

Polymer modification processes like graft polymerization or “polymer-analogous” transformations can lead to microstructure modifications in polymers, impacting shape and thermal stability. Advanced analytical techniques can identify and describe these microstructures at low concentrations, revealing intricate moieties. For example, this dissertation reveals the presence of 1,3-bis(2-chloroethyl) branch structures in PVC that were previously undetectable. These microstructures significantly influence the shape and thermal stability of polymeric materials.

The model number of the SEM used in this study was

JSM-IT210 (Jeol, Tokyo, Japan). Specifications were as follows: electron high tension = 15.00 kV, working distance = 9.0 mm, signal type = Type I secondary electrons, magnification = 100 kx. PVC, initially thick with a particle structure and microparticles, undergoes significant structural changes after chemical modification, forming lamellar zones with tiny flakes and porous structures. Chemical treatment alters PVC’s inherent structure and expands its surface area, making it useful as an adsorbent due to its ability to change its structure (Figure 1). Chitosan (Cs) is generated by insufficient deacetylation of chitin. β -(1,4)-2-acetamino-2-deoxy-D-glucose and β -(1,4)-2-amino-2-deoxy-D-glucose are among its constituents, along with a noteworthy quantity of amino and hydroxyl groups that aid in forming robust connections with nanoparticles or other polymer chains to produce a novel mixture possessing enhanced properties. N-vinyl pyrrolidone monomer polymerization yields polyvinyl pyrrolidone (PVP), a hydrophilic polymer. For this reason, in the polymeric matrix, Cs, and PVP are exactly matched. The polymers are miscible due to the hydrogen bond attraction between the hydroxyl and amino groups of Cs and the carbonyl groups associated with PVP. In order to compare this composite to the AuNPs embedded in the HEMA composite (test), it was determined that it was an ideal internal standard (IS) for X-ray diffraction (XRD) tests. 50 mg of AuNPs were scraped off a pure gold strip, and 1 mg of AuNPs was taken successively with 3, 7, 10, and 20 mL (AuNPs-3, AuNPs-7, AuNPs-10, and AuNPs-20), respectively, to prepare the concentration. The prepared AuNPs concentration in HEMA will be tested on XRD against IS Cs/PVP.

For X-ray powder diffraction (XRPD) analysis of dust intakes, Malvern Panalytical’s XRD solutions (Malvern, United Kingdom) were utilized in this study. This method was used to examine the microstructure of materials composed of polycrystalline bacteria. Additionally, an FT/IR-6X Fourier transform infrared spectroscopy (FTIR) spectrometer (Jasco, Easton, USA) equipped with a HgCdTe photovoltaic (MCT-PV) detector was used to perform the gold coat film entrapment tests with colony density in this study. The measurement wavenumber range of this instrument is 25000 ~ 20 cm^{-1} . Regarding the sample chamber, its dimensions are 200 × 260 × 185 mm (width × depth × height). This instrument serves as a means for identifying the variable-angle FTIR transmittance measurement with polarization, as well as conducting the protein secondary structure analysis of bacterial release in low-concentration aqueous solutions.

Table 2. Comparative Screening Evaluation Reports of Designed Extra Nasal Cone (NC-1) with Designed Masks in Market

Screening Device/Tools	Scattered Size Distribution and Concentration of Atmospheric Particles and Microbes through Pneumatic Screening Phenomena			Residuals	Remark
	Zone just after Entering the Nasal Cone [A]/Outside Layer of a Mask	Zone in the Middle of the Nasal Cone [B]/Middle Layer of a Mask	Zone just at the End of the Slide into the Chamber [C]/Inner Side Layer of a Mask		
NC-1	80 ~ 95%	10 ~ 15%	5 ~ 7%	$\leq 0.2 \mu\text{m}$ Non-Sticky Particles	Highly Safest
DL2	60%	20%	20%	$\leq 0.5 \mu\text{m}$ Non-Sticky Particles	Moderate Safe
DL3	62%	18%	21%	$\leq 0.5 \mu\text{m}$ Non-Sticky Particles	Moderate Safe
DS2	61%	17%	18%	$\leq 0.5 \mu\text{m}$ Non-Sticky Particles	Moderate Safe
DS3	65%	15%	12%	$\leq 0.5 \mu\text{m}$ Non-Sticky Particles	Safest
FFP2	67%	17%	19%	$\leq 0.5 \mu\text{m}$ Non-Sticky Particles	Moderate Safe
FFP3	63%	17%	17%	$\leq 0.5 \mu\text{m}$ Non-Sticky Particles	Moderate Safe
KN100	71%	20%	13%	$\leq 0.5 \mu\text{m}$ Non-Sticky Particles	Moderate Safe
KP95 and KP100	60%	13%	16%	$\leq 0.5 \mu\text{m}$ Non-Sticky Particles	Moderate Safe
P2	68%	16%	18%	$\leq 0.5 \mu\text{m}$ Non-Sticky Particles	Moderate Safe
P3	64%	16%	19%	$\leq 0.5 \mu\text{m}$ Non-Sticky Particles	Moderate Safe
PPF2	66%	12%	19%	$\leq 0.5 \mu\text{m}$ Non-Sticky Particles	Moderate Safe
PPF3	69%	11%	10%	$\leq 0.5 \mu\text{m}$ Non-Sticky Particles	Safe
R95	73%	13%	12%	$\leq 0.5 \mu\text{m}$ Non-Sticky Particles	Safe

2.9. Clinical Investigation

Throughout the COVID era, the incidence and prevalence of the illness state were carefully tracked, and it became clear how crucial the design, application, and filtration of the mask are. Multi-layered masks must be secured firmly in order to provide protection from coughed aerosol and particle pollutants present in the atmosphere (Das et al., 2021). Therefore, it disrupted the blood flow to the face, resulting in hypoxia. The mask has one flaw despite having several layers of fabric. The tiny breathing hole might let bio-pathogens and certain dust particles through (Ogbuaji et al., 2021). In this study, a total of 50 volunteers were divided into three separate groups: seniors (74%), athletes (16%), and young adults (10%) for the open study. The investigation was conducted both before and after the mask was worn (Table 1). The objective of this investigation is to determine the decrease in discomfort linked to the signs and symptoms, and the effectiveness of the mask depending on the force exposure. Therefore, it becomes necessary to facilitate breathing and offer 99% filtering of outside air. Conical filtration was created to filter the air inside cone filtration assemblies to achieve this objective. Clinical studies have also been performed to assure efficient filtering and removal from the nasal cone filter.

3. Results and Discussion

Incorporating DG into PET has not been investigated because DG is not suitable for processing at high temperatures (Ahmad et al., 2014). Therefore, in this study, DG was treated with to prepare reinforced DG (RDG), which was then used as a biological filler that was melt-mixed with a PET resin to produce PET/DG and PET/RDG composites. The composite mechanical properties were investigated. Compared with PET/DG composites, PET/RDG composites exhibited improved mechanical properties (Guo et al., 2021). When the RDG content

was 12.5%, the elongation at break reached the maximum (Yao et al., 2020). SEM was used to observe the structure of composites filled with MDI modified DG at the tensile section. Meanwhile, the compatibility between RDG fillers and the PET matrix was analyzed. RDG dispersed and adhered well in the matrix (Tsou et al., 2023). The centripetal and axial shelves of the nasal cone, which was made of PC materials as the septum frame and grooves of gold metal micro-granules, received a thin film coating of HEMA plasticizer.

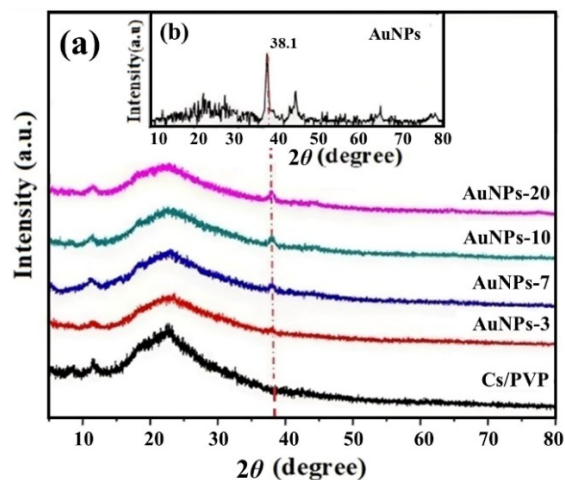


Figure 6. XRD spectra of (a) AuNPs in various volumes with Cs/PVP and (b) the integral average diffraction peaks with noise associated with AuNPs only at the 2θ (degree) curve.

Clinical studies were conducted to assess the impact of COVID-related force exposure on different demographics, including senior citizens, young athletes, and normal youth. The study aimed to determine the average recurrence rates of respiratory diseases or SARS-CoV-2, breathlessness, cardiovascular

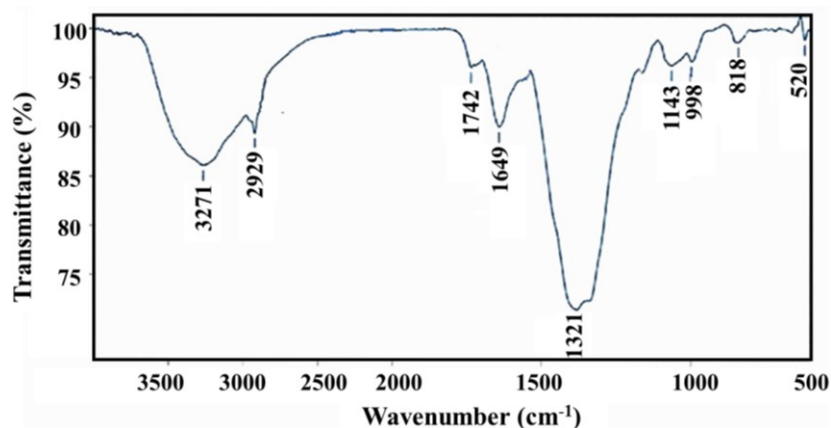


Figure 7. Comparative bacterial colony on AuNPs HEMA as per the concentration-based transmittance interference vs wavenumbers cm^{-1} .

diseases (CVD), allergic reactions, nasopharyngeal discomfort, and immediate communicable disease retardation. Results showed reductions in average recurrence rates to 22, 36, and 0% for senior citizens, young athletes, and normal youth, respectively. Estimates of particle size and viable bioactive microbial quantitation were made within the 50 individuals (Table 2). Additionally, the results are self-product validated by swabbing random samples from various regions of the suggested integral mask.

The performance of the extra nasal cone (NC-1) screening was compared to that of disposable level 2 (DL2), disposable level 3 (DL3), disposable surgical 3 (DS3), filtering facepiece particles 2 (FFP2), filtering facepiece particles 3 (FFP3), Korean standard 100 (KN100), Korean standard particulate 95 (KP95), particulate 2 (P2), particulate 3 and filtering facepiece particles 2 (P3PFF2), particulate filtering facepiece 3 (PFF3), respirator 95 (R95), and other screens. According to the results, there are fewer airborne particles and germs spread out across zones A (i.e., zone just after entering the nasal cone), B (i.e., zone in the middle of the nasal cone), C (i.e., zone just at the end of the slide into the chamber), and D (i.e., zone at the nasal cone). It was remarked that the additional nasal cone, which filtered particles smaller than 200 nm, was the safest.

Through XRD (Figure 6), the density of AuNPs layer coatings was found in varied volumes at the same concentration. Therefore, the size of the metallic crystallized surface area could be calculated. The XRD exhibits a peak of 38.9 at 2 (degree). As a result, the AuNPs HEMA film gold layer coat is connected to a microcrystalline size that is specific to the layer-by-layer, multi-fold adsorption of microbiological pollutants. Additionally, it is helpful for quick elimination after washing. Microbe differentiation was identified with FTIR. The FTIR results showed the appearance of new characteristic peaks, indicating the possibility of DG reacting with MDI after the blending with PET. These layers of gold capture a variety of bacterial species, which may be identified using structural analysis and molecular size. Higher wave lengths result in lower frequencies, and vice versa, according to a relationship between transmittance and wavenumber. Figure 7 indicates that different airborne mi-

crobes are confined in the device and exhibit decreased transmittance. A trough with a 1321 wavenumber was shown to be the cause of the high zone collecting affinity of bacteria. The reduced bacterial colony concentration is reflected in several different troughs.

4. Conclusions

This study reveals the relative superiority of the suitable high-tech design of the AuNPs HEMA composite mask over the other mentioned masks. The in-vitro mechanical mode test of the design and implementation of AuNP coated biocompatible polymeric matrix mesh plasticizers implanted on PVC plastic porous grid was successful. This is made to be reusable for microbial screening to fend off pandemics, ensure lab safety, and even fight against biological warfare. Therefore, this innovative approach to mask design represents a potential advancement in public health and safety during pandemics and other infectious disease outbreaks. Further research and development may continue to refine and improve this novel screening mask design.

Acknowledgements. This work was enlightened by the attentive consideration of final year Pharm. D students at Sagar University, Bangalore, as clinical concurrent patient investigation as well as retrospective data interpretation of Sagar Hospital, Bangalore. The laboratory data were obtained using X-ray diffractometer in the radiotherapy lab at Sagar Medical College Labs and FTIR from the pharmaceutical analysis lab at the Department of Pharmaceutical Sciences.

References

- Abd-Elsayed, A. and Karri, J. (2020). Utility of substandard face mask options for health care workers during the COVID-19 pandemic. *Anesthesia and Analgesia*. 131(1), 4-6. <https://doi.org/10.1213/ANE.0000000000004841>
- Ahmad, J. Kalim, D., Muddasar, Habib. and Hägg, M.B. (2014). Influence of TiO_2 nanoparticles on the morphological, thermal and solution properties of PVA/ TiO_2 nanocomposite membranes. *Arabian Journal for Science and Engineering*. 39, 6805-6814. <https://doi.org/10.1007/s13369-014-1287-0>

- Akovi, G. (2012). Plastic materials: Polyvinyl chloride (PVC). *Toxicity of Building Materials*. 23-53. <https://doi.org/10.1533/9780857096357.23>
- Allison, A.L., Esther, A.D., Maria, B., Arredondo, M.C., Chau, C., Chandler, K., Dobrijevic, D., Aparasi, T.D., Hailes, H.C., Lettieri, P., Liu, C., Medda, F., Michie, S., Miodownik, M., Munro, B., Purkiss, D. and John M. Ward (2021). The impact and effectiveness of the general public wearing masks to reduce the spread of pandemics in the UK: A multidisciplinary comparison of single-use masks versus reusable face masks. *UCL Open Environment*. 3, e022. <https://doi.org/10.14324/111.444/ucloe.000022>
- Armentano, I., Barbanera, M., Carota, E., Crognale, S., Marconi, M., Rossi, S., Rubino, G., Scungio, M., Taborri, J. and Calabro, G. (2021). Polymer materials for respiratory protection: Processing, end use, and testing methods. *ACS Applied Polymer Materials*. 3, 531-548. <https://doi.org/10.1021/acscapm.0c01151>
- Atangana, E. and Atangana, A. (2020). Facemasks simple but powerful weapons to protect against COVID-19 spread: Can they have side effects? *Results in Physics*. 19, 103425. <https://doi.org/10.1016/j.rinp.2020.103425>
- Chen, S.C., Fu, X.H., Jing, Z.J. and Chen, H.Z. (2022). Non-isothermal crystallization kinetics and rheological behaviors of PBT/PET blends: Effects of PET property and nano-silica content. *Designed Monomers and Polymers*. 25, 32-46. <https://doi.org/10.1080/15685551.2022.2041784>
- Chou, R., Dana, T. and Jungbauer, R. (2022). Update alert 8: Masks for prevention of respiratory virus infections, including SARS-CoV-2, in health care and community settings. *Annals of Internal Medicine*. 175, W108-W09. <https://doi.org/10.7326/L22-0272>
- Chou, R., Dana, T., Jungbauer, R., Weeks, C. and McDonagh, M.S. (2020). Masks for prevention of respiratory virus infections, including SARS-CoV-2, in health care and community settings: A living rapid review. *Annals of Internal Medicine*. 173, 542-555. <https://doi.org/10.7326/M20-3213>
- Clase, C.M., Fu, E.L., Joseph, M., Beale, R.C.L., Dolovich, M.B., Jardine, M., Mann, J.F.E., Pecoits-Filho, R., Winkelmayer, W.C. and Carrero, J.J. (2020). Cloth masks may prevent transmission of COVID-19: an evidence-based, risk-based approach. *American College of Physicians*. 173(6), 489-491. <https://doi.org/10.7326/M20-2567>
- Das, S., Sarkar, S., Das, A., Das, S., Chakraborty, P. and Sarkar, J. (2021). A comprehensive review of various categories of face masks resistant to Covid-19. *Clinical Epidemiology and Global Health*. 12, 100835. <https://doi.org/10.1016/j.cegh.2021.100835>
- Edwards, K.L. (1998). A designers' guide to engineering polymer technology. *Materials and Design*. 19(1-2), 57-67. [https://doi.org/10.1016/S0261-3069\(98\)00009-0](https://doi.org/10.1016/S0261-3069(98)00009-0)
- Emblem, A. (2012). 13 - Plastics properties for packaging materials. *Packaging Technology*. 287-309. <https://doi.org/10.1533/9780857095701.2.287>
- Gandhi, N.R., Moll, A., Sturm, A.W., Pawinski, R., Govender, T., Lalloo, U., Zeller, K., Andrews, J. and Friedland, G. (2006). Extensively drug-resistant tuberculosis as a cause of death in patients co-infected with tuberculosis and HIV in a rural area of South Africa. *Lancet*. 368, 1575-1580. [https://doi.org/10.1016/S0140-6736\(06\)69573-1](https://doi.org/10.1016/S0140-6736(06)69573-1)
- Gelmanova, I.Y., Keshavjee, S., Golubchikova, V.T., Berezina, V.I., Strelis, A.K., Yanova, G.V., Atwood, S. and Murray, M. (2007). Barriers to successful tuberculosis treatment in Tomsk, Russian Federation: Non-adherence, default and the acquisition of multidrug resistance. *Bulletin of the World Health Organization*. 85, 703-711. <https://doi.org/10.2471/BLT.06.038331>
- Grignoli, N., Petrocchi, S., Bernardi, S., Massari, I., Traber, R., Malacrida, R. and Gabutti, L. (2021). Influence of empathy disposition and risk perception on the psychological impact of lockdown during the coronavirus disease pandemic outbreak. *Frontiers in Public Health*. 8, 567337. <https://doi.org/10.3389/fpubh.2020.567337>
- Guo, J.P., Tsou, C.H., De Guzman, M.R., Wu, C.S., Zhang, X.M., Chen, Z.J., Wen, Y.H., Yang, T., Zhuang, Y.J., Ge, F.F., Chen, Z.J. and Wang, Z.H. (2021). Preparation and characterization of bio-based green renewable composites from poly(lactic acid) reinforced with corn stover. *Journal of Polymer Research*. 28, 199. <https://doi.org/10.1007/s10965-021-02559-1>
- Hutten, I.M. (2016). *Handbook of Nonwoven Filter Media (2nd Edition)*. Butterworth Heinemann. 1-650. <https://doi.org/10.1016/C2011-0-05753-8>
- Jefferson, T., Foxlee, R., Del Mar, C., Dooley, L., Ferroni, E., Hewak, B., Prabhala, A., Nair, S. and Rivetti, A. (2008). Physical interventions to interrupt or reduce the spread of respiratory viruses: systematic review. *British Medical Journal*. 336, 77-80. <https://doi.org/10.1136/bmj.39393.510347.BE>
- Krzeminski, P., Tomei, M.C., Karaolia, P., Langenhoff, A., Almeida, C.M.R., Felis, E., Gritten, F., Andersen, H.R., Fernandes, T., Manaia, C.M., Rizzo, L. and Fatta-Kassinos, D. (2019). Performance of secondary wastewater treatment methods for the removal of contaminants of emerging concern implicated in crop uptake and antibiotic resistance spread: A review. *Science of the Total Environment*. 648, 1052-1081. <https://doi.org/10.1016/j.scitotenv.2018.08.130>
- Kumar, S. and Parekh, S.H. (2020). Linking graphene-based material physicochemical properties with molecular adsorption, structure and cell fate. *Communications Chemistry*. 3, 8. <https://doi.org/10.1038/s42004-019-0254-9>
- Lin, Z.Z., Wang, Z., Zhang, X. and Diao, D.F. (2021). Superhydrophobic, photo-sterilize, and reusable mask based on graphene nanosheet-embedded carbon (GNEC) film. *Nano Research*. 14, 1110-1115. <https://doi.org/10.1007/s12274-020-3158-1>
- Loeb, M., Bartholomew, A., Hashmi, M., Tarhuni, W., Hassany, M., Youngster, I., Somayaji, R., Larios, O., Kim, J., Missaghi, B., Vayalumkal, J.V., Mertz, D., Chagla, Z., Cividino, M., Ali, K., Mansour, S., Castellucci, L.A., Frenette, C., Parkes, L., Downing, M., Muller, M., Glavin, V., Newton, J., Hookoom, R., Leis, J.A., Kinross, J., Smith, S., Borhan, S., Singh, P., Pullenayegum, E. and Conly, J. (2022). Medical masks versus N95 respirators for preventing COVID-19 among health care workers: A randomized trial. *Annals of Internal Medicine*. 175(12), 1629-1638. <https://doi.org/10.7326/M22-1966>
- MacIntyre, C.R., Chughtai, A.A., Rahman, B., Peng, Y., Zhang, Y., Seale, H., Wang, X.L. and Wang, Q.Y. (2017). The efficacy of medical masks and respirators against respiratory infection in healthcare workers. *Influenza and Other Respiratory Viruses*. 11, 511-517. <https://doi.org/10.1111/irv.12474>
- Neupane, B.B., Mainali, S., Sharma, A. and Giri, B. (2019). Optical microscopic study of surface morphology and filtering efficiency of face masks. *PeerJ*. 7, e7142. <https://doi.org/10.7717/peerj.7142>
- O'Donnell, M.R., Jarand, J., Loveday, M., Padayatchi, N., Zelnick, J., Werner, L., Naidoo, K., Master, I., Osburn, G., Kvasnovsky, C., Shean, K., Pai, M., Van der Walt, M., Horsburgh, C.R. and Dheda, K. (2010). High incidence of hospital admissions with multidrug-resistant and extensively drug-resistant tuberculosis among South African health care workers. *Annals of Internal Medicine*. 153, 516-522. <https://doi.org/10.7326/0003-4819-153-8-201010190-00008>
- OECD (2020). *The face mask global value chain in the COVID-19 outbreak: Evidence and policy lessons*. Organisation for Economic and Development. <https://www.oecd.org/coronavirus/policy-responses/the-face-mask-global-value-chain-in-the-COVID-19-outbreak-evidence-and-policy-lessons-a4df866d/> (accessed May 04, 2020).
- Offeddu, V., Yung, C.F., Low, M.S.F. and Tam, C.C. (2017). Effectiveness of masks and respirators against respiratory infections in healthcare workers: A systematic review and meta-analysis. *Clinical Infectious Diseases*. 65, 1934-1942. <https://doi.org/10.1093/cid/cix681>

- Ogbuoji, E.A., Zaky, A.M. and Escobar, I.C. (2021). Advanced research and development of face masks and respirators pre and post the coronavirus disease 2019 (COVID-19) pandemic: A critical review. *Polymers*. 13(12), 1998. <https://doi.org/10.3390/polym13121998>
- Pang, Z.J., Zhao, Y., Luo, N.Q., Chen, D.H. and Chen, M. (2022). Flexible pressure and temperature dual-mode sensor based on buckling carbon nanofibers for respiration pattern recognition. *Scientific Reports*. 12, 17434. <https://doi.org/10.1038/s41598-022-21572-y>
- Rengasamy, S., Sbarra, D., Nwoko, J. and Shaffer, R. (2015). Resistance to synthetic blood penetration of National Institute for Occupational Safety and Health-approved N95 filtering facepiece respirators and surgical N95 respirators. *American Journal of Infection Control*. 43(11), 1190-1196. <https://doi.org/10.1016/j.ajic.2015.06.014>
- Rosner, E. (2020). Adverse effects of prolonged mask use among healthcare professionals during COVID-19. *Journal of Infectious Diseases and Epidemiology*. 6, 130. <https://doi.org/10.23937/2474-3658/1510130>
- Smith, J.D., MacDougall, C.C., Johnstone, J., Copes, R.A., Schwartz, B. and Garber, G.E. (2016). Effectiveness of N95 respirators versus surgical masks in protecting health care workers from acute respiratory infection: A systematic review and meta-analysis. *Canadian Medical Association Journal*. 188(8), 567-754. <https://doi.org/10.1503/cmaj.150835>
- Stearne, J.M. and Ward, I.M. (1969). The tensile behaviour of polyethylene terephthalate. *Journal of Materials Science*. 4, 1088-1096. <https://doi.org/10.1007/BF00549849>
- Tsou, C.H., Ma, Z.L., Yang, T., De Guzman, M.R., Chen, S., Wu, C.S., Hu, X.F., Huang, X., Sun, Y.L., Gao, C., Zhao, W.B. and Zeng, C.Y. (2023). Reinforced distiller's grains as bio-fillers in environment-friendly poly(ethylene terephthalate) composites. *Polymer Bulletin*. 80, 6137-6158. <https://doi.org/10.1007/s00289-022-04318-8>
- Ullah, S., Ullah, A., Lee, J., Jeong, Y., Hashmi, M., Zhu, C., Joo, K.I., Cha, H.J. and Kim, I.S. (2020). Reusability comparison of melt-blown vs nanofiber face mask filters for use in the coronavirus pandemic. *ACS Applied Nano Materials*. 3(7), 7231-7241. <https://doi.org/10.1021/acsnano.0c01562>
- Yang, R.X., Zhang, W.Q., Tiwari, N., Yan, H., Li, T.J. and Cheng, H.Y. (2022). Multimodal sensors with decoupled sensing mechanisms. *Advanced Science*. 9(26), 2202470. <https://doi.org/10.1002/advs.202202470>
- Yao, Y.L., De Guzman, M.R., Duan, H., Gao, C., Lin, X., Wen, Y.H., Du, J., Lin, L., Chen, J.C., Wu, C.S., Suen, M.C., Sun, Y.L., Hung, W.S. and Tsou, C.H. (2020). Infusing high-density polyethylene with graphene-zinc oxide to produce antibacterial nanocomposites with improved properties. *Chinese Journal of Polymer Science*. 38(8), 898-907. <https://doi.org/10.1007/s10118-020-2392-z>
- Ye, Z.L., Ling, Y., Yang, M.Y., Xu, Y.D., Zhu, L., Yan, Z. and Chen, P.Y. (2022). A breathable, reusable, and zero-power smart face mask for wireless cough and mask-wearing monitoring. *ACS Nano*. 16, 5874-5884. <https://doi.org/10.1021/acsnano.1c1041>
- Zhang, Y., Chu, D.F., Zheng, M.Y., Kissel, T. and Agarwal, S. (2012). Biocompatible and degradable poly(2-hydroxyethyl methacrylate) based polymers for biomedical applications. *Polymer Chemistry*. 3, 2752-2759. <https://doi.org/10.1039/C2PY20403G>